Supporting Information

Highly Stable Lanthanide(III) Metal-organic Frameworks as Ratiometric Fluorescence Sensors for Vitamin B_6

Xiao-Qing Wang[a,c*], Jiandong Yang[a], Man Zhang[a], Dan Wu[a], Tuoping Hu[a,c] and Jie Yang[b*]

[a] Department of Chemistry, College of Science, North University of China, Taiyuan 030051, China.

[b] Shandong Provincial Key Laboratory of Chemical Energy Storage and Novel Cell Technology, and School of Chemistry and Chemical Engineering, Liaocheng University, Liaocheng 252000, China.

[c] Shanxi Key Laboratory of advanced carbon based electrode materials, North University of China, Taiyuan 030051, China

EXPERIMENTAL SECTION

Materials and General Methods. All materials and chemicals are purchased and used without further purification. Human serum was purchased from AmyJet Scientific Inc. , which was diluted 20 times with deionized water for use. The organic ligand 1,1′-ethynebenzene-3,3′,5,5′ -tetracarboxylic acid (**H_4EBTC**) was purchased from Jilin Yanshen Technology Co. , Ltd and 2-Fluorobenzoic acid was purchased from Shanghai Aladdin Biochemical Technology Co., Ltd. Thermogravimetric analyses (TGA) were tested using a ZCT-A analyzer under nitrogen atmosphere within 25-800 °C region. FTIR-8400S spectrometer was used to record Fourier transform infrared (IR) spectroscopy at the rang of the 4000-400 cm^{-1}. UV-2600 spectrophotometer was used to record UV-vis absorption spectra. X-ray photoelectron spectroscopy (XPS) experiment was performed on a Thermo ESCALAB 250XI. Elemental analyses including C, H were measured using Vario MACRO cube elemental analyzer. Photoluminescence spectrum was obtained through Hitachi F-4600 fluorescence spectrophotometer. The overall photoluminescence quantum yields were obtained on an integrating sphere covered with barium sulfate at room temperature.[s1] The Gas-sorption isotherms were carried out on the surface area analyzer ASAP-2020.

Preparation of Ln-MOFs@SA hydrogel [Ln=Eu (1), Tb (2)]. Taking complex **1**@SA as an example, the suspension of complex **1** was prepared to dispersed complex **1** (1.5 mg) powder in deionized water (1 mL) by ultrasonic method. Deionized water (20 mL) was heated to boiling, and then sodium alginate (SA) powder (1.0 g) was dissolved in the boiling water to form SA solution. Drop 0.25 mL SA solution into the suspension and stir continuously for 1 h to form complex **1**@SA. The mixture was poured into the purchased mold and cooled to room temperature to form the complex **1**@SA hydrogel.

Preparation of Ln-MOFs@SA film [Ln=Eu (1), Tb (2)]. The prepared complex **1**@SA hydrogel was heated and dried in an oven at 80 °C for 2 h to obtain the complex **1**@SA film.

Fluorescence detection of vitamin B_6. The fluorescence properties of the complexes **1** and **2** suspension with different analytes were studied at room temperature. Taking complex **1** as an example, the **1** suspension was prepared by adding 1.0 mg of the **1** powder sample to 2.0 mL of phosphate buffer solutions (PBS, pH=7.35) of different analytes (0.010 $mol \cdot L^{-1}$), including proline

(Pro), glycine (Gly), glutamine (Gln), leucine (Leu), methionine (Met), phenylalanine (Phe), histidine (His), threonine (Thr), asparaginic acid (Asp), cysteine (Cys), asparagine (Asn), valine (Val), isoleucine (Ile), vitamin C (VC), vitamin B_1 (VB_1), vitamin B_6 (VB_6), glutataione (GSH), uric acid (UA), ultrasonicating the solution for 30 min, and placing it overnight to let it form a uniform emulsion.

Fluorescence titration experiment. Taking complex **1** as an example, the 1.0 mg powder of **1** was dispersed in 2 mL solution of the target analytes at different concentrations.

Fluorescence determination of recovery experiment. Taking complex **1** as an example, the powder of **1** was centrifuged from the suspension, washed (three times with deionized water) and dried. Then it was added again to the target analyte to determine its fluorescence performance. The above operation was repeated five times.

Time-varying flourescence sensing experiment. Taking complex **1** as an example, the fluorescence spectra of **1** in VB_6 (0.005 M) PBS buffer were recorded within 6 min.

Sensing of vitamin B_6 in human serum. Taking complex **1** as an example, 10 μL of human serum (diluted by 20 fold) was added to an aqueous solution of 1 mg·L^{-1} complex **1**, and then sonicate for 15 min to obtained a stable suspension. A series of vitamin B_6 PBS buffer with different concentrations were added to the suspension to record its fluorescence spectra.

Table S1 Crystal data for complexes **1-3**.

Complexes	**1**	**2**	**3**
Formula	$C_{27}H_{19}Eu_3O_{19}$	$C_{27}H_{19}Tb_3O_{19}$	$C_{27}H_{19}Ce_3O_{19}$
M_r	1103.33	1124.18	1067.78
pace group	*R-3c*	*R-3c*	*R-3c*
a (Å)	17.6167(6)	17.6231(8)	17.9267(4)
b (Å)	17.6167(6)	17.6231(8)	17.9267(4)
c (Å)	49.2103(14)	48.762(2)	49.8631(16)
α (deg)	90	90	90
β deg)	90	90	90
γ (deg)	120	120	120
Z	12	12	12
V (Å^3)	13226.3(9)	13115.3(13)	13877.5(8)
D_c (g cm^{-3})	1.635	1.708	1.508
μ (mm^{-1})	30.674	24.001	22.931
F (000)	6156.0	6336.0	5974.0
no. of unique reflns	9306	14436	15818
no. of obsd reflns [$I>2\sigma(I)$]	2628	2975	3105
Parameters	144	149	149
GOF	1.063	0.880	1.084
Final *R* indices [$I>2\sigma(I)$]^{a,b}	R_1=0.0634 wR_2=0.1632	R_1= 0.0559, wR_2= 0.1533	R_1= 0.0980, wR_2= 0.2499

R indices (all data)	R_1=0.0.0671	R_1= 0.0711,	R_1=0.1129
	wR_2=0.1662	wR_2= 0.1630	wR_2=0.2629
ρ_{max}/ρ_{min} (e Å^{-3})	2.56 and -5.70	1.21 and -1.06	2.39 and -1.44

$^{a}R_1 = \sum ||F_o| - |F_c|| / \sum |F_o|$. $^{b}wR_2 = [\sum w(F_o^2 - F_c^2)^2 / \sum w(F_o^2)^2]^{0.5}$.

Table S2 Selected bond lengths (Å) and angles (o) for complexes **1-3**.

Complex **1**

Eu1—Eu1^{i}	3.9990 (9)	O5^{i}—Eu1—Eu1^{ii}	158.06 (15)
Eu1—Eu1^{ii}	3.9581 (9)	O5^{i}—Eu1—Eu1^{iii}	102.44 (15)
Eu1—Eu1^{iii}	3.9581 (9)	O5^{i}—Eu1—Eu1^{i}	68.88 (15)
Eu1—O4	2.376 (6)	O5^{i}—Eu1—O6^{iv}	77.0 (2)
Eu1—O5^{i}	2.404 (6)	O5^{i}—Eu1—H2	133.2
Eu1—O6^{iv}	2.409 (7)	O5^{i}—Eu1—H1	59.6
Eu1—O7^{v}	2.365 (7)	O5^{i}—Eu1—O3	66.5 (2)
Eu1—O2	2.366 (3)	O6^{iv}—Eu1—Eu1^{i}	108.84 (19)
Eu1—H2	2.7127	O6^{iv}—Eu1—Eu1^{iii}	69.62 (18)
Eu1—O1	2.364 (6)	O6^{iv}—Eu1—Eu1^{ii}	105.81 (18)
Eu1—O1^{vi}	2.387 (6)	O6^{iv}—Eu1—H2	62.7
Eu1—O1^{ii}	2.367 (6)	O6^{iv}—Eu1—H1	66.3
Eu1—H1	2.7044	O6^{iv}—Eu1—O3	65.1 (2)
Eu1—O3	2.619 (7)	O7^{v}—Eu1—Eu1^{ii}	67.99 (19)
Eu1^{iii}—Eu1—Eu1^{ii}	60	O7^{v}—Eu1—Eu1^{iii}	107.1 (2)
Eu1^{iii}—Eu1—Eu1^{i}	60.339 (8)	O7^{v}—Eu1—Eu1^{i}	157.91 (19)
Eu1^{ii}—Eu1—Eu1^{i}	90	O7^{v}—Eu1—O4	84.9 (2)
Eu1^{ii}—Eu1—H2	43.2	O7^{v}—Eu1—O5^{i}	133.2 (2)
Eu1^{i}—Eu1—H2	101.6	O7^{v}—Eu1—O6^{iv}	80.3 (3)
Eu1^{iii}—Eu1—H2	43.2	O7^{v}—Eu1—H2	63.9
Eu1^{ii}—Eu1—H1	100.9	O7^{v}—Eu1—O1^{ii}	75.7 (2)
Eu1^{iii}—Eu1—H1	43	O7^{v}—Eu1—O1^{vi}	137.3 (2)
Eu1^{i}—Eu1—H1	42.5	O7^{v}—Eu1—H1	140.7
O4—Eu1—Eu1^{i}	101.52 (14)	O7^{v}—Eu1—O3	66.9 (2)
O4—Eu1—Eu1^{iii}	156.96 (15)	O2—Eu1—Eu1^{iii}	33.22 (10)
O4—Eu1—Eu1^{ii}	109.45 (15)	O2—Eu1—Eu1^{i}	86.3 (2)
O4—Eu1—O5^{i}	81.6 (2)	O2—Eu1—Eu1^{ii}	33.22 (10)
O4—Eu1—O6^{iv}	132.9 (2)	O2—Eu1—O4	142.44 (17)
O4—Eu1—H2	143.6	O2—Eu1—O5^{i}	134.38 (15)
O4—Eu1—O1^{vi}	72.8 (2)	O2—Eu1—O6^{iv}	75.8 (3)
O4—Eu1—H1	133	O2—Eu1—O7^{v}	76.3 (3)
O4—Eu1—O3	67.9 (2)	O2—Eu1—H2	17.6
O2—Eu1—O1^{vi}	99.8 (3)	O1^{vi}—Eu1—H1	74.9
O2—Eu1—O1^{ii}	65.7 (2)	O1—Eu1—O3	130.6 (2)
O2—Eu1—H1	76	O1^{ii}—Eu1—O3	130.8 (2)

O2—Eu1—O3	129.4 (3)	O1^{vi}—Eu1—O3	130.8 (2)
H2—Eu1—H1	82.1	O3—Eu1—Eu1^{iii}	134.69 (15)
O1—Eu1—Eu1^{iii}	33.22 (15)	O3—Eu1—Eu1^{i}	135.16 (15)
O1^{ii}—Eu1—Eu1^{iii}	85.47 (15)	O3—Eu1—Eu1ii	134.84 (15)
O1^{vi}—Eu1—Eu1^{ii}	85.51 (15)	O3—Eu1—H2	111.8
O1^{vi}—Eu1—Eu1^{iii}	85.55 (15)	O3—Eu1—H1	112.9
O1—Eu1—Eu1^{ii}	85.50 (15)	C9—O4—Eu1	130.2 (6)
O1—Eu1—Eu1^{i}	32.87 (15)	C9—O5—Eu1^{vi}	127.6 (6)
O1^{ii}—Eu1—Eu1^{ii}	33.19 (15)	C1—O6—Eu1^{viii}	135.3 (7)
O1^{vi}—Eu1—Eu1^{i}	32.57 (15)	C1—O7—Eu1^{ix}	139.4 (7)
O1^{ii}—Eu1—Eu1^{i}	84.86 (15)	Eu1—O2—Eu1^{ii}	113.6 (2)
O1^{ii}—Eu1—O4	78.4 (2)	Eu1—O2—Eu1^{iii}	113.6 (2)
O1—Eu1—O4	133.5 (2)	Eu1^{ii}—O2—Eu1^{iii}	113.6 (2)
O1^{ii}—Eu1—O5i	142.9 (2)	Eu1—O2—H2	105
O1—Eu1—O5^{i}	73.6 (2)	Eu1^{iii}—O2—H2	105
O1^{vi}—Eu1—O5^{i}	79.7 (2)	Eu1^{ii}—O2—H2	105
O1^{vi}—Eu1—O6^{iv}	140.9 (2)	Eu1—O1—Eu1^{iii}	113.6 (3)
O1^{ii}—Eu1—O6^{iv}	138.3 (2)	Eu1—O1—Eu1^{i}	114.6 (2)
O1—Eu1—O6^{iv}	78.8 (2)	Eu1^{iii}—O1—Eu1^{i}	114.5 (2)
O1—Eu1—O7^{v}	140.0 (3)	Eu1—O1—H1	104.5
O1—Eu1—O2	65.7 (2)	Eu1^{i}—O1—H1	103.4
O1—Eu1—H2	76.2	Eu1^{iii}—O1—H1	104.5
O1^{ii}—Eu1—H2	76.1	Eu1—O3—H3A	127.6
O1^{vi}—Eu1—H2	117.4	Eu1—O3—H3B	127.7
O1—Eu1—O1^{vi}	64.7 (2)	C2—C1—O6—Eu1^{viii}	−172.8 (8)
O1—Eu1—O1^{ii}	98.6 (3)	C2—C1—O7—Eu1^{ix}	164.0 (8)
O1^{ii}—Eu1—O1^{vi}	64.6 (2)	O6—C1—O7—Eu1^{ix}	−14 (2)
O1^{ii}—Eu1—H1	116.3	O7—C1—O6—Eu1^{viii}	4.9 (19)
O1—Eu1—H1	17.7		

Symmetry codes: (i) y, −x+y, −z+1; (ii) −y, x−y, z; (iii) −x+y, −x, z; (iv) −y+2/3, −x+1/3, z−1/6; (v) x−1/3, x−y+1/3, z−1/6; (vi) x−y, x, −z+1; (vii) −x+1, −y+1, −z+1; (viii) −y+1/3, −x+2/3, z+1/6; (ix) x+1/3, x−y+2/3, z+1/6.

Complex **2**

Tb1—Tb1^{i}	3.9203 (8)	O3—Tb1—O6	130.3 (4)
Tb1—Tb1^{ii}	3.9203 (8)	O3—Tb1—O5^{v}	75.9 (2)
Tb1—Tb1^{iii}	3.9548 (8)	O3—Tb1—O7^{vi}	76.0 (2)
Tb1—O2	2.355 (4)	O1^{iii}—Tb1—Tb1^{ii}	109.51 (16)
Tb1—O2^{iii}	2.343 (5)	O1^{iii}—Tb1—Tb1^{i}	157.47 (15)
Tb1—O2^{iv}	2.357 (5)	O1^{iii}—Tb1—Tb1^{iii}	68.01 (16)
Tb1—O4	2.376 (6)	O1^{iii}—Tb1—O4	82.1 (2)
Tb1—O3	2.342 (2)	O1^{iii}—Tb1—O6	66.1 (4)
Tb1—O1^{iii}	2.364 (6)	O1^{iii}—Tb1—O5^{v}	132.3 (2)

Tb1—O6	2.67 (2)	O6—Tb1—Tb1^{i}	136.0 (4)
Tb1—O5^{v}	2.370 (6)	O6—Tb1—Tb1^{ii}	134.6 (4)
Tb1—O7^{vi}	2.339 (6)	O6—Tb1—Tb1^{iii}	134.0 (4)
Tb1^{ii}—Tb1—Tb1^{iii}	60.286 (8)	O5^{v}—Tb1—Tb1^{i}	69.72 (15)
Tb1^{ii}—Tb1—Tb1^{i}	60	O5^{v}—Tb1—Tb1^{iii}	159.64 (15)
Tb1^{i}—Tb1—Tb1^{iii}	90	O5^{v}—Tb1—Tb1^{ii}	105.73 (17)
O2^{iv}—Tb1—Tb1^{iii}	85.14 (12)	O5^{v}—Tb1—O4	76.5 (2)
O2^{iii}—Tb1—Tb1^{i}	85.95 (12)	O5^{v}—Tb1—O6	66.3 (4)
O2^{iv}—Tb1—Tb1^{i}	33.36 (12)	O7^{vi}—Tb1—Tb1^{iii}	104.99 (17)
O2—Tb1—Tb1^{iii}	32.94 (12)	O7^{vi}—Tb1—Tb1^{i}	106.85 (18)
O2—Tb1—Tb1^{i}	85.76 (12)	O7^{vi}—Tb1—Tb1^{ii}	67.59 (17)
O2—Tb1—Tb1^{ii}	85.97 (13)	O7^{vi}—Tb1—O2^{iv}	139.9 (2)
O2^{iii}—Tb1—Tb1^{iii}	32.75 (11)	O7^{vi}—Tb1—O2	137.3 (2)
O2^{iv}—Tb1—Tb1^{ii}	85.77 (12)	O7^{vi}—Tb1—O4	133.3 (2)
O2^{iii}—Tb1—Tb1^{ii}	33.59 (12)	O7^{vi}—Tb1—O1^{iii}	84.5 (2)
O2^{iii}—Tb1—O2	65.03 (16)	O7^{vi}—Tb1—O6	67.0 (5)
O2^{iii}—Tb1—O2^{iv}	99.3 (2)	O7^{vi}—Tb1—O5^{v}	80.3 (2)
O2—Tb1—O2^{iv}	64.82 (15)	Tb1^{iv}—O2—Tb1^{iii}	113.1 (2)
O2—Tb1—O4	79.77 (19)	Tb1^{iv}—O2—Tb1	114.68 (19)
O2^{iii}—Tb1—O4	143.27 (19)	Tb1—O2—Tb1^{iii}	114.15 (19)
O2^{iv}—Tb1—O4	73.27 (19)	Tb1^{iv}—O2—H2	104.5
O2—Tb1—O1^{iii}	73.15 (19)	Tb1—O2—H2	104.5
O2^{iii}—Tb1—O1^{iii}	78.1 (2)	Tb1^{iii}—O2—H2	104.5
O2^{iv}—Tb1—O1^{iii}	134.07 (19)	C7—O4—Tb1	127.7 (5)
O2^{iii}—Tb1—O6	129.3 (5)	Tb1^{ii}—O3—Tb1^{i}	113.63 (15)
O2^{iv}—Tb1—O6	131.4 (5)	Tb1—O3—Tb1^{ii}	113.63 (15)
O2—Tb1—O6	129.6 (4)	Tb1—O3—Tb1^{i}	113.63 (15)
O2^{iii}—Tb1—O5^{v}	138.5 (2)	Tb1—O3—H3	104.9
O2—Tb1—O5^{v}	141.0 (2)	Tb1^{ii}—O3—H3	104.9
O2^{iv}—Tb1—O5^{v}	78.8 (2)	Tb1^{i}—O3—H3	104.9
O2^{iii}—Tb1—O7^{vi}	75.2 (2)	C7—O1—Tb1^{iv}	128.8 (6)
O4—Tb1—Tb1^{i}	102.23 (15)	Tb1—O6—H6A	127.3
O4—Tb1—Tb1^{iii}	110.76 (16)	Tb1—O6—H6B	127.3
O4—Tb1—Tb1^{ii}	158.18 (15)	C9—O5—Tb1^{v}	135.9 (6)
O4—Tb1—O6	66.7 (5)	C9—O7—Tb1^{viii}	140.0 (6)
O3—Tb1—Tb1^{ii}	33.19 (8)	Tb1—O4—C7—O1	57.0 (12)
O3—Tb1—Tb1^{iii}	86.24 (16)	Tb1—O4—C7—C3	−123.9 (7)
O3—Tb1—Tb1^{i}	33.19 (8)	Tb1^{iv}—O1—C7—O4	−61.0 (12)
O3—Tb1—O2^{iii}	66.06 (16)	Tb1^{iv}—O1—C7—C3	119.9 (8)
O3—Tb1—O2^{iv}	65.84 (16)	Tb1^{v}—O5—C9—C2	−174.1 (7)
O3—Tb1—O2	100.1 (2)	Tb1^{v}—O5—C9—O7	6.0 (16)
O3—Tb1—O4	134.07 (15)	Tb1^{viii}—O7—C9—C2	164.4 (7)
O3—Tb1—O1^{iii}	142.44 (17)	Tb1^{viii}—O7—C9—O5	−15.8 (16)

Symmetry codes: (i) −x+y+1, −x+2, z; (ii) −y+2, x−y+1, z; (iii) x−y+1, x, −z+1; (iv) y, −x+y+1, −z+1;

(v) −x+4/3, −x+y+2/3, −z+7/6; (vi) x−y+4/3, −y+5/3, −z+7/6; (vii) −x+1, −y+2, −z+1; (viii) x−y+1/3, −y+5/3, −z+7/6.

Complex **3**

Ce1—Ce1^{i}	4.0942 (12)	O3—Ce1—O7^{vi}	75.5 (4)
Ce1—Ce1^{ii}	4.1352 (11)	O4—Ce1—Ce1^{ii}	100.6 (2)
Ce1—Ce1^{iii}	4.0943 (12)	O4—Ce1—Ce1i	155.8 (2)
Ce1—O2^{iii}	2.455 (8)	O4—Ce1—Ce1^{iii}	108.9 (2)
Ce1—O2	2.439 (8)	O4—Ce1—O1	68.3 (4)
Ce1—O2^{iv}	2.457 (8)	O4—Ce1—O5^{ii}	81.7 (3)
Ce1—O3	2.438 (4)	O4—Ce1—O6^{v}	134.9 (3)
Ce1—O4	2.464 (9)	O4—Ce1—O7^{vi}	86.6 (4)
Ce1—O1	2.644 (12)	O1—Ce1—Ce1^{i}	135.4 (4)
Ce1—O5^{ii}	2.493 (10)	O1—Ce1—Ce1^{ii}	135.0 (3)
Ce1—O6^{v}	2.489 (9)	O1—Ce1—Ce1^{iii}	135.0 (3)
Ce1—O7^{vi}	2.466 (10)	O5^{ii}—Ce1—Ce1^{iii}	157.5 (2)
Ce1^{iii}—Ce1—Ce1^{ii}	89.999 (1)	O5^{ii}—Ce1—Ce1^{ii}	68.2 (2)
Ce1^{i}—Ce1—Ce1^{iii}	60	O5^{ii}—Ce1—Ce1^{i}	102.3 (2)
Ce1^{i}—Ce1—Ce1^{ii}	60.327 (10)	O5^{ii}—Ce1—O1	67.0 (4)
O2—Ce1—Ce1^{iii}	85.37 (19)	O6^{v}—Ce1—Ce1^{ii}	107.9 (3)
O2—Ce1—Ce1^{ii}	32.51 (17)	O6^{v}—Ce1—Ce1^{i}	68.6 (3)
O2^{iv}—Ce1—Ce1^{iii}	85.17 (18)	O6^{v}—Ce1—Ce1^{iii}	105.4 (2)
O2^{iii}—Ce1—Ce1^{iii}	33.09 (18)	O6^{v}—Ce1—O1	66.8 (5)
O2—Ce1—Ce1^{i}	33.34 (19)	O6^{v}—Ce1—O5^{ii}	77.5 (3)
O2^{iii}—Ce1—Ce1^{ii}	84.52 (18)	O7^{vi}—Ce1—Ce1^{iii}	66.9 (3)
O2^{iii}—Ce1—Ce1^{i}	85.17 (18)	O7^{vi}—Ce1—Ce1^{ii}	156.8 (3)
O2^{iv}—Ce1—Ce1^{i}	85.41 (19)	O7^{vi}—Ce1—Ce1^{i}	105.8 (3)
O2^{iv}—Ce1—Ce1^{ii}	32.66 (18)	O7^{vi}—Ce1—O1	68.2 (4)
O2—Ce1—O2^{iii}	97.9 (4)	O7^{vi}—Ce1—O5^{ii}	134.9 (4)
O2^{iii}—Ce1—O2^{iv}	64.1 (2)	O7^{vi}—Ce1—O6^{v}	80.7 (4)
O2—Ce1—O2^{iv}	64.3 (2)	Ce1—O2—Ce1^{i}	113.6 (3)
O2^{iii}—Ce1—O4	77.9 (3)	Ce1—O2—Ce1^{ii}	115.3 (3)
O2—Ce1—O4	132.4 (3)	Ce1^{i}—O2—Ce1^{ii}	114.6 (3)
O2^{iv}—Ce1—O4	71.8 (3)	Ce1^{i}—O2—H2	103.8
O2^{iii}—Ce1—O1	130.8 (4)	Ce1^{ii}—O2—H2	103.8
O2^{iv}—Ce1—O1	130.4 (4)	Ce1—O2—H2	103.8
O2—Ce1—O1	131.2 (4)	Ce1^{iii}—O3—Ce1^{i}	114.2 (2)
O2^{iv}—Ce1—O5^{ii}	79.4 (3)	Ce1^{i}—O3—Ce1	114.2 (2)
O2^{iii}—Ce1—O5^{ii}	142.1 (3)	Ce1^{iii}—O3—Ce1	114.2 (2)
O2—Ce1—O5^{ii}	73.3 (3)	Ce1^{iii}—O3—H3	104.2
O2^{iii}—Ce1—O6^{v}	138.0 (3)	Ce1^{i}—O3—H3	104.2
O2^{iv}—Ce1—O6^{v}	140.2 (3)	Ce1—O3—H3	104.2
O2—Ce1—O6^{v}	78.2 (3)	C9—O4—Ce1	131.8 (9)
O2^{iii}—Ce1—O7^{vi}	75.4 (3)	Ce1—O1—H1A	127.5

O2—Ce1—O7^{vi}	138.9 (3)	Ce1—O1—H1B	128
O2^{iv}—Ce1—O7^{vi}	137.0 (3)	C9—O5—Ce1^{iv}	127.5 (9)
O3—Ce1—Ce1^{iii}	32.90 (12)	C1—O6—Ce1^{viii}	137.3 (9)
O3—Ce1—Ce1^{ii}	85.6 (3)	C1—O7—Ce1^{ix}	141.2 (10)
O3—Ce1—Ce1^{i}	32.90 (12)	Ce1—O4—C9—O5	60 (2)
O3—Ce1—O2	65.3 (3)	Ce1—O4—C9—C6	−118.5 (13)
O3—Ce1—O2^{iv}	98.7 (4)	Ce1^{iv}—O5—C9—O4	−56.9 (19)
O3—Ce1—O2^{iii}	65.1 (3)	Ce1^{iv}—O5—C9—C6	121.3 (13)
O3—Ce1—O4	141.7 (3)	C2—C1—O6—Ce1^{viii}	174.4 (11)
O3—Ce1—O1	130.9 (5)	C2—C1—O7—Ce1^{ix}	−167.8 (12)
O3—Ce1—O5^{ii}	134.2 (2)	O6—C1—O7—Ce1^{ix}	13 (3)
O3—Ce1—O6^{v}	75.8 (3)	O7—C1—O6—Ce1^{viii}	−6 (3)

Symmetry codes: (i) −y+2, x−y+1, z; (ii) x−y+1, x, −z+1; (iii) −x+y+1, −x+2, z; (iv) y, −x+y+1, −z+1; (v) −y+5/3, −x+4/3, z−1/6; (vi) −x+y+2/3, y+1/3, z−1/6; (vii) −x+1, −y+1, −z+1; (viii) −y+4/3, −x+5/3, z+1/6; (ix) −x+y+1/3, y−1/3, z+1/6.

Table S3 The CIE coordinates of doped **Eu_xTb_{1-x}-MOFs**.

	EU/%	**TB/%**	**CIE**
EU_XTB_{1-X}-MOFS	100	0	0.5574, 0.3125
	90	10	0.5468, 0.3089
	80	20	0.5417, 0.3111
	70	30	0.5590, 0.3267
	60	40	0.5760, 0.3359
	50	50	0.5272, 0.3355
	40	60	0.4634, 0.3597
	30	70	0.3934, 0.4136
	20	80	0.3876, 0.4302
	10	90	0.3236, 0.4729
	0	100	0.2518, 0.5348

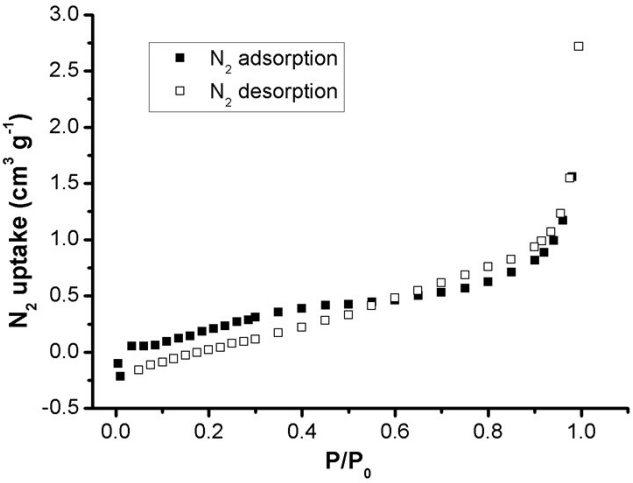

Fig. S1 The N_2 adsorption−desorption isotherms of complex **1**.

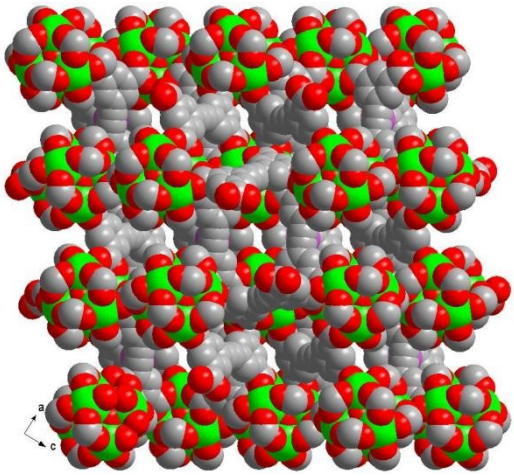

Fig. S2 The 3D porous framework for **1** shown in the space-filling mode along *b* axis.

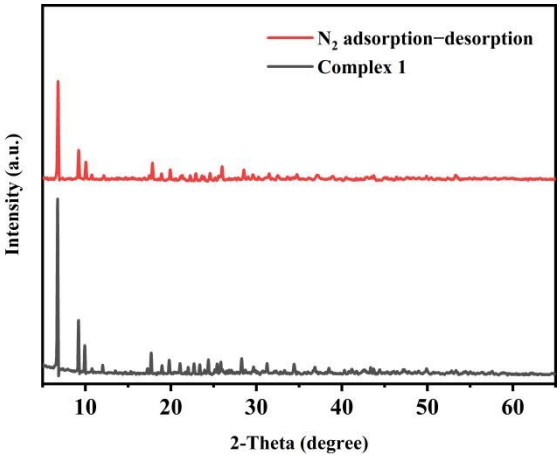

Fig. S3 The PXRD patterns of complex **1** after adsorption N_2.

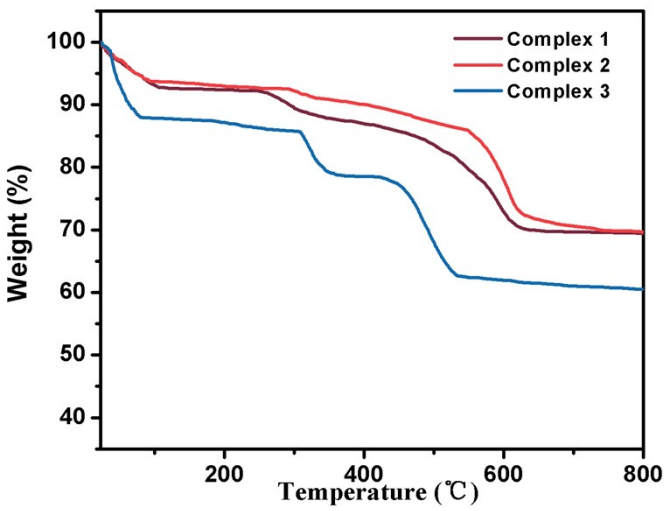

Fig. S4 The TGA curves of complexes **1-3**.

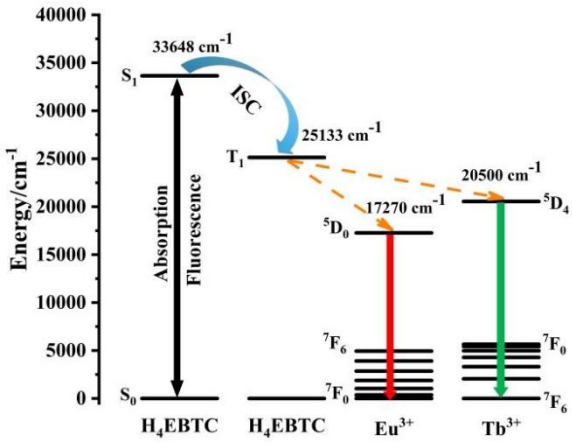

Fig. S5 Energy transfer in the complexes **1** and **2**.

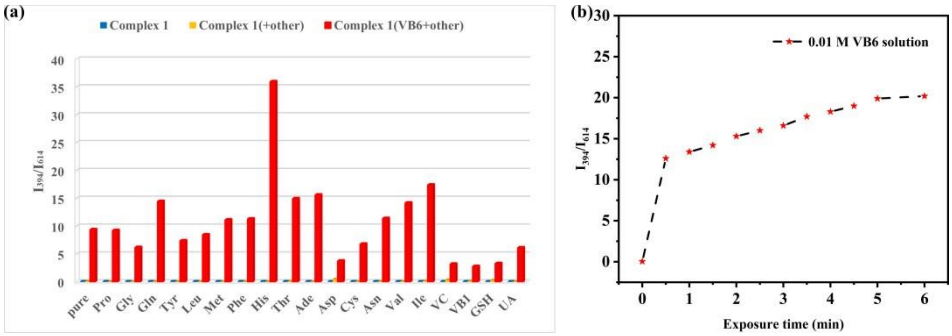

Fig. S6 (a)The I_{394}/I_{614} value of complex **1** under the present of VB_6 and interference analytes. (b) The influence of reaction time on fluorescence intensity of complex **1**.

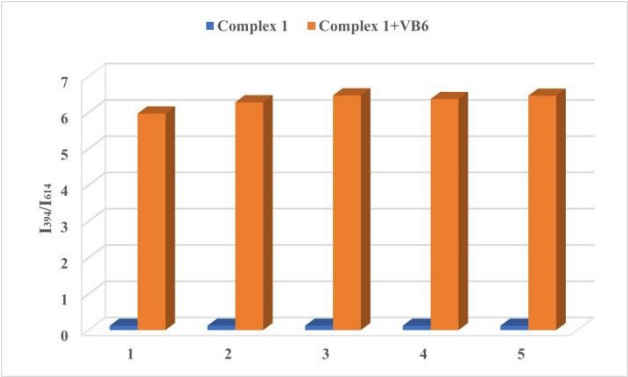

Fig. S7 The fluorescence intensity ratio of complex **1** for detecting VB_6 after five cycles.

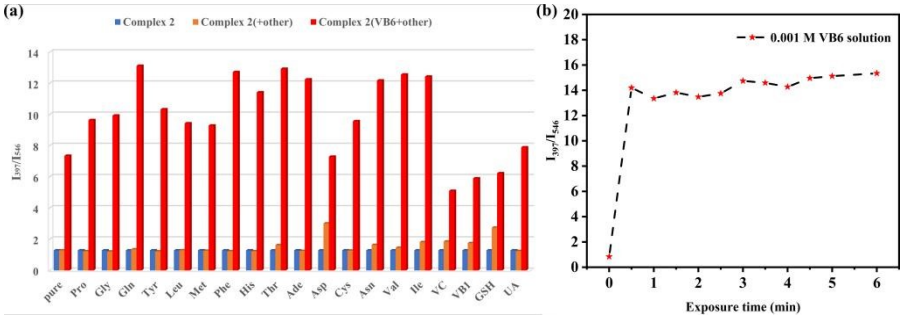

Fig. S8 (a) The I_{394}/I_{614} value of complex **2** under the present of VB_6 and interference analytes. (b) The influence of reaction time on fluorescence intensity of complex **2**.

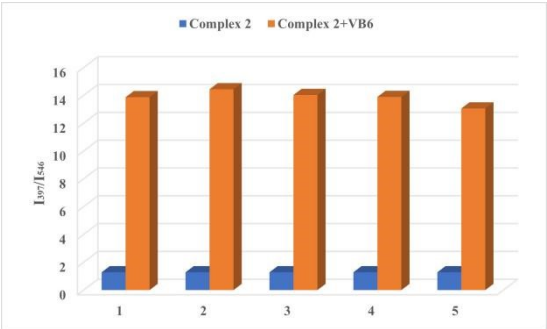

Fig. S9 The fluorescence intensity ratio of complex **2** for detecting VB_6 after five cycles.

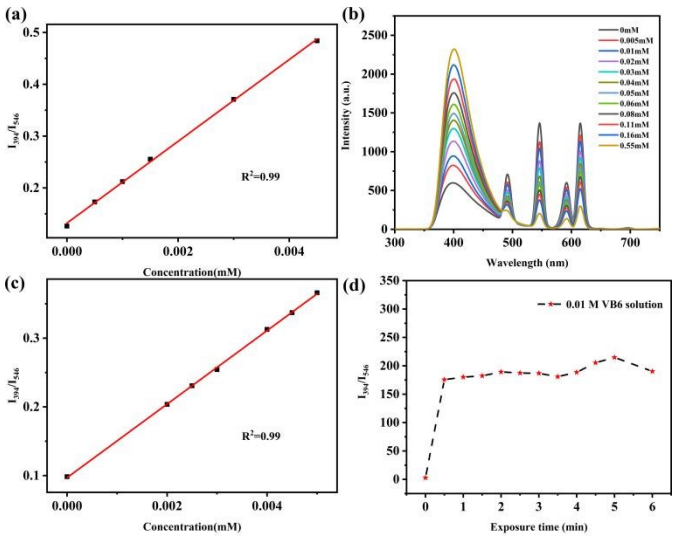

Fig. S10 (a) Linear fitting relationship of **Eu_2Tb_8-MOF** between fluorescence intensity ratio I_{394}/I_{546} and VB_6 concentration. (b) The fluorescence emission spectra of **Eu_2Tb_8-MOF** with the addition of VB_6 in phosphate buffer solution including 10 μL of human serum. (c) Linear fitting relationship of **Eu_2Tb_8-MOF** between fluorescence intensity ratio I_{394}/I_{546} and VB_6 concentration in phosphate buffer solution including 10 μL of human serum. (d) The influence of reaction time on fluorescence intensity of **Eu_2Tb_8-MOF**.

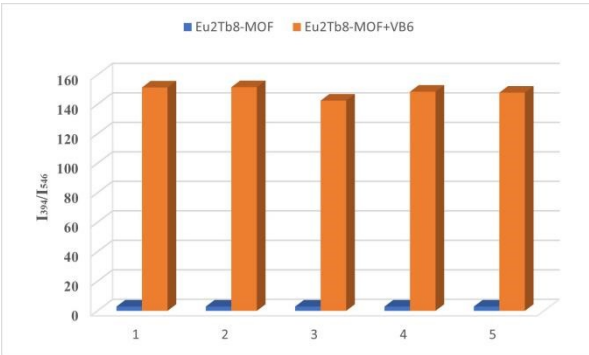

Fig. S11 The fluorescence intensity ratio of **Eu_2Tb_8-MOF** for detecting VB_6 after five cycles.

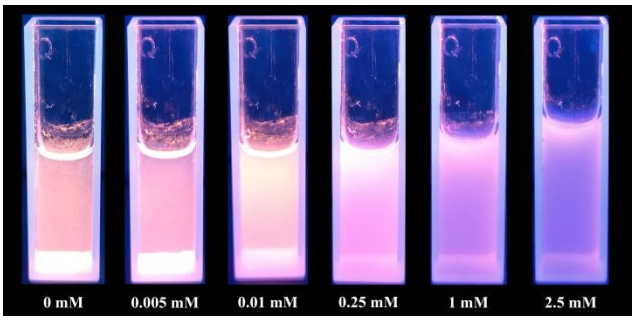

Fig. S12 The fluorescence color of Eu_2Tb_8-MOF under 254 nm UV-vis lamp with VB_6 concentration of 0, 0.005, 0.01, 0.25, 1, 2.5 mM.

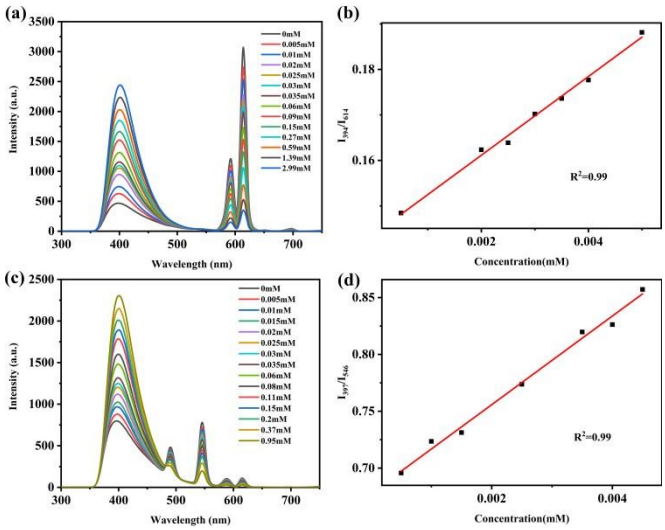

Fig. S13 (a) The fluorescence emission spectra of complex **1** with the addition of VB_6 in phosphate buffer solution including 10 μL of human serum. (b) Linear fitting relationship between fluorescence intensity ratio I_{394}/I_{614} and VB_6 concentration. (c) The fluorescence emission spectra of complex **2** with the addition of VB_6 in phosphate buffer solution including 20 μL of human serum. (d) Linear fitting relationship between fluorescence intensity ratio I_{397}/I_{546} and VB_6 concentration.

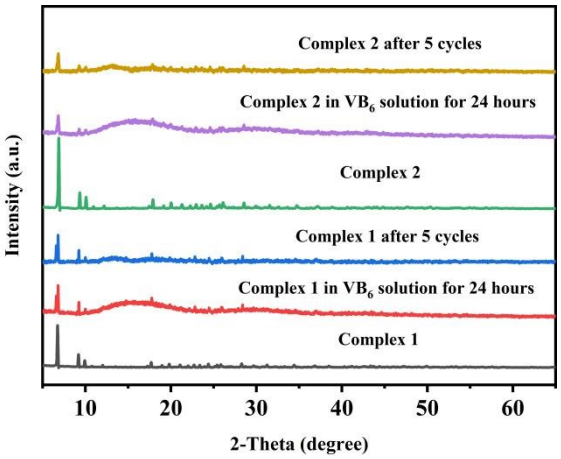

Fig. S14 The PXRD patterns of complexes **1** and **2** after detection of VB_6 for 24 h and complexes **1** and **2** detecting VB_6 after five cycles.

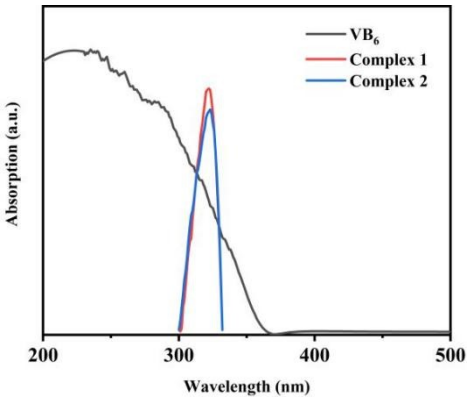

Fig. S15 The UV-vis absorption spectra of VB_6, and the excitation spectra of complexes **1** and **2**.

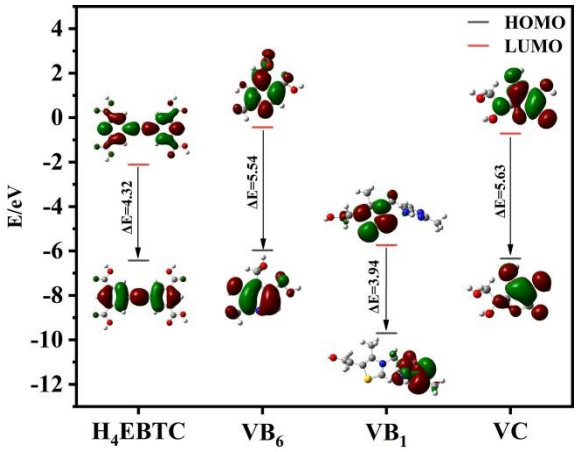

Fig. S16 LUMO and HOMO energy levels of H_4EBTC and three vitamins.

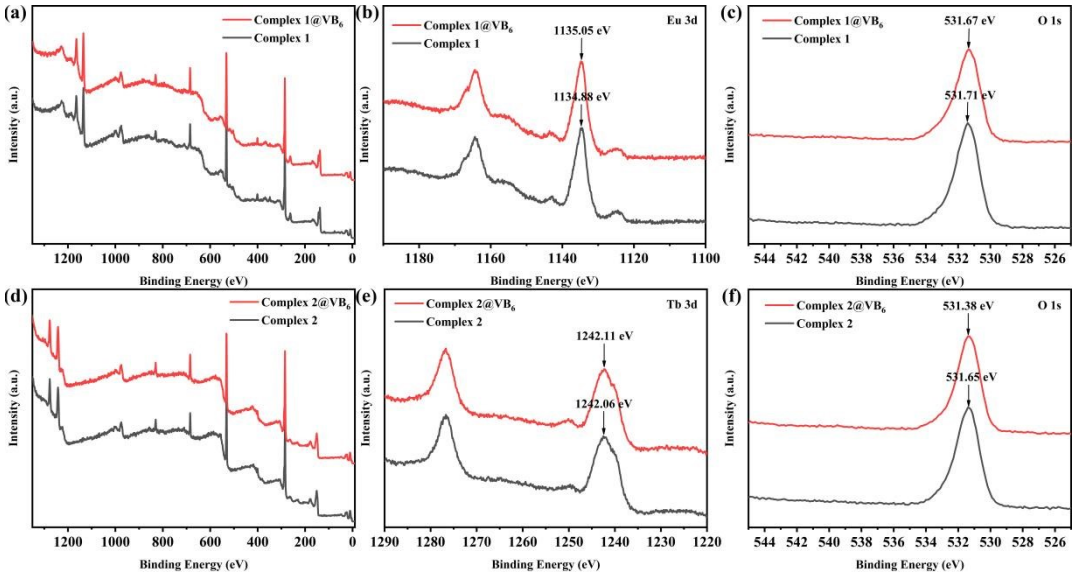

Fig. S17 (a) XPS spectra of complex **1**, complex **1@VB$_6$**. (b) Eu 3d for complex **1**, complex **1@VB$_6$**. (c) O 1s for complex **1**, complex **1@VB$_6$**. (d) XPS spectra of complex **2**, complex **2@VB$_6$**. (e) Tb 3d for complex **2**, complex **2@VB$_6$**. (f) O 1s for complex **2**, complex **2@VB$_6$**.

Reference

S1 X. -N. Mi, D. -F. Sheng, Y. -E. Yu, Y. -H. Wang, L. -M. Zhao, J. Lu, Y. -W. Li, D. -C. Li, J. -M. Dou, J. -G. Duan and S. -N. Wang, *ACS Appl. Mater. Interfaces*, 2019, **11**, 7914–7926.